

Quaking Neutron Stars

Lucia M. Franco¹

University of Chicago, 5640 S. Ellis Ave., Chicago IL 60637; lucia@oddjob.uchicago.edu

Bennett Link¹

Montana State University, Department of Physics, Bozeman MT 59717;

blink@dante.physics.montana.edu

and

Richard I. Epstein

Los Alamos National Laboratory, Mail Stop D436, Los Alamos, NM 87545;

epstein@lanl.gov

Received _____; accepted _____

¹Also Los Alamos National Laboratory

ABSTRACT

Gravitational, magnetic and superfluid forces can stress the crust of an evolving neutron star. Fracture of the crust under these stresses could affect the star’s spin evolution and generate high-energy emission. We study the growth of strain in the crust of a spinning down, magnetized neutron star and examine the initiation of crust cracking (a *starquake*). In preliminary work (Link, Franco & Epstein 1998), we studied a homogeneous model of a neutron star. Here we extend this work by considering a more realistic model of a solid, homogeneous crust afloat on a liquid core. In the limits of astrophysical interest, our new results qualitatively agree with those from the simpler model: the stellar crust fractures under shear stress at the rotational equator, matter moves to higher latitudes and the star’s oblateness is reduced. Magnetic stresses favor faults directed toward the magnetic poles. Thus our previous conclusions concerning the star’s spin response still hold; namely, asymmetric redistribution of matter excites damped precession which could ultimately lead to an increase in the spin-down torque. Starquakes associated with glitches could explain the permanent *offsets* in period derivative observed to follow glitches in at least three pulsars.

Subject headings: dense matter — magnetic fields — stars: magnetic fields — stars: neutron — pulsars: individual (Crab)

1. Introduction

Stresses developing in the crust of an evolving neutron star could fracture the crust (*i.e.* a starquake), possibly affecting the star’s spin evolution and generating high-energy emission. Spin down (*e.g.*, in isolated pulsars; Baym & Pines 1971) or spin up (*e.g.*, in accreting neutron stars) changes the equilibrium shape of the star, building stresses. In “magnetars”, decay of the superstrong field ($B \gtrsim 10^{14}$ G) could break the crust and produce episodes of intense gamma-ray emission (Thompson & Duncan 1996; Thompson & Blaes 1998). Differential rotation between the crust and the interior neutron superfluid may also stress the crust to its breaking point (Ruderman 1976).

Starquake-induced rearrangement of the star’s mass distribution changes the star’s moment of inertia causing precession and polar wandering (Link, Franco & Epstein 1998; hereafter LFE). Anomalous spin behavior might therefore signal the occurrence of a starquake. Such evidence for crust cracking may already exist in several isolated pulsars. Permanent *offsets* in period derivative following glitches have been observed in the Crab pulsar (Lyne, Pritchard, & Smith 1993), PSR1830-08 and probably PSR0355+54 (Shemar & Lyne 1996). The observed offsets all have the same sign, and correspond to increases in spin-down rate. In LFE we interpreted these offsets as due to permanent increases in the torque acting on the neutron star. We showed that cracking and readjustment of the stellar crust in response to the star’s slow down can increase the angle between the star’s spin and magnetic axes, leading to an increase in the spin-down torque in some models of pulsar spin down.

Other evidence for cracking of the neutron star crust can be found in the Soft Gamma Repeaters, thought to be strongly magnetized neutron stars ($B \gtrsim 10^{14}$ G), or *magnetars*. Unlike radio pulsars which have weaker magnetic fields and are powered by rotation, magnetars are thought to be powered by their intense magnetic fields. Duncan & Thompson

(1994; also Thompson & Duncan 1995; 1996) have suggested that SGR outbursts represent cracking of the crust by magnetic stresses. Evidence in favor of this hypothesis is the striking statistical similarities between bursts in SGRs and earthquakes (Cheng *et al.* 1996; Gogus *et al.* 1999). For both phenomena the energy released per event obeys similar power-law scalings and the waiting times between events are strongly correlated with one another.

The potential importance of violent crust dynamics in neutron star evolution motivates this detailed study of spin-down induced starquakes. The equilibrium shape for a spinning star is an oblate spheroid which becomes more spherical as the star slows down. The liquid core is able to change its shape smoothly as the star slows down. In contrast, the solid crust is strained as it evolves through a continuous series of equilibrium configurations, and eventually will crack if it is brittle. In LFE, we modeled the neutron star as a homogeneous, self-gravitating, elastic sphere and followed the evolution of strain in its crust as the star spins down. From our calculations we developed the following picture of starquakes. Crust cracking occurs as equatorial material shears under the compressive forces arising from the star’s decreasing circumference. The star’s oblateness suddenly decreases as matter moves to higher latitudes along a slip or *fault* plane that is perpendicular to the stellar surface and crosses the equator at an angle of $\sim 30 - 45^\circ$ (see Fig. 6). Since magnetic stresses suppress shearing near the magnetic poles and across the field lines, starquakes likely originate near the two points on the equator farthest from the magnetic poles and propagate preferentially toward the magnetic poles. The matter redistribution breaks the rotational symmetry of the star, causing the star to precess. Damping of the precession eventually restores alignment between the angular velocity and angular momentum, ultimately *increasing* the angle between the spin axis and the magnetic moment. In some models of pulsar spin-down (*e.g.*, the vacuum-dipole model) an increase in the alignment angle between the rotation and magnetic axes increases the spin-down torque. The magnitude of the starquake-induced

changes in the alignment angle are consistent with the changes in the spin-down rates seen in the Crab pulsar (LFE). The observations of spin-down offsets in coincidence with glitches indicates some connection between structural readjustments and glitches. For a recent discussion of this possibility, see Link & Epstein (1996).

In this paper we extend the analysis to the more realistic case of a brittle shell floating on a liquid core. We find that the stresses induced by the star’s spin down produce similar behavior to that found in LFE. Crust cracking associated with other sources of stress, such as magnetic or superfluid stresses, will be considered in future work. The organization of this paper is as follows. Section 2 presents a qualitative description of the growth and release of strain in the crust of an idealized, spinning-down neutron star. In §3, we calculate the response of the crust’s shape as it spins down, treating the star as a homogeneous solid afloat on a liquid core. In §4, we explore the cracking and matter flow for a model with realistic crust thickness. In §5 we discuss the effects of a magnetic field anchored in the crust. Section 6 summarizes our results.

2. Growth and Release of Strain in a Spinning-down Star

Our analysis is based on the assumption that the neutron star crust is brittle, and therefore cracks when sufficiently strained². We consider a neutron star spinning with

²Experience with terrestrial materials shows that material properties at high pressure can differ from those at low pressure. For example, terrestrial materials typically become ductile when subjected to pressures in excess of their shear moduli. Nevertheless, deep-focus earthquakes are known to originate from regions of very high pressure (Green & Houston 1995). These faults are thought to be triggered by densification phase changes; small regions of higher density nucleate as the material is stressed, and act as a lubricant for shearing

angular velocity Ω which undergoes a change $-\delta\Omega$ in its rotation rate where $0 < \delta\Omega \ll \Omega$. Our goal is to describe the effects on the star’s crust resulting from this change in rotation rate. In equilibrium, the star has a spheroidal shape with an equatorial bulge of relative size $\sim (\Omega R/v_k)^2$ where R is the radius of the non-rotating configuration and v_k is the Keplerian velocity. As the star spins down, the fluid interior readjusts its shape continuously, following (in the homogeneous case) a sequence of Maclaurin spheroids (see, *e.g.*, Chandrasekhar, S. 1987; p.77). As the solid crust attempts to readjust its shape, however, strain builds. Material originally at \mathbf{r} is displaced to $\mathbf{r} + \mathbf{u}(\mathbf{r})$, where $\mathbf{u}(\mathbf{r})$ is the *displacement field*. The local distortion of the solid is given by the *strain tensor* (see, *e.g.*, Landau & Lifshitz 1959; p.3)

$$u_{ij} = \frac{1}{2} \left(\frac{\partial u_i}{\partial x_j} + \frac{\partial u_j}{\partial x_i} \right). \quad (1)$$

In a local coordinate system in which this matrix is diagonal, the eigenvalues ϵ_{ii} represent compression ($\epsilon_{ii} < 0$) or dilation ($\epsilon_{ii} > 0$) along the respective axes. Let the largest and smallest eigenvalues be ϵ_l and ϵ_s , respectively. The *strain angle* is $\epsilon_l - \epsilon_s$, and we refer to the plane containing the corresponding principal axes as the *stress plane*. In Fig. 1 we show schematically a block of matter that is compressed along the y direction and allowed to expand along the z direction. The stress plane then is parallel to the $y - z$ plane.

The elastic limit of the matter is reached first in the regions of the crust where the strain angle is maximum. There the material cracks, forming a fault plane perpendicular to the stress plane (Fig. 1). Matter slips along the fault plane and redistributes in a way that reduces the equatorial circumference, thus releasing the strain. The fracture geometry depends on where the strain angle is maximum and how its value changes over the crust.

motion. Analogous processes might occur in the high-pressure material of the neutron star. E. Ramirez-Ruiz and R. I. Epstein are examining whether the phase transition from spherical nuclei to rod-like nuclei may facilitate starquakes.

We now turn to a calculation of the spin-down induced strain in the neutron star crust.

3. Matter Redistribution in a Spinning-down Star

To explore the accumulation and release of strain in a slowing neutron star, we model the star as a two-component homogeneous spheroid; a self-gravitating core of incompressible liquid on which rests a crust of uniform density. The non-rotating configuration is a sphere of core radius R' and total radius R .

3.1. Equilibrium Equations

A spinning, self-gravitating object has an equilibrium configuration given by

$$\nabla \cdot \mathbf{T} - \rho \nabla \phi = \mathbf{F}, \quad (2)$$

where \mathbf{T} is the material stress tensor, ϕ is the gravitational potential per unit mass and \mathbf{F} is the centrifugal force density associated with the rotation. For rigid material, strain develops as the force is changed. The strain in the material is given by the strain tensor of eq. (1). For incompressible matter we have

$$\nabla \cdot \mathbf{u} = u_{ii} = 0, \quad (3)$$

where repeated indices indicate sums.

For sufficiently small strains, the material can be described using Hooke's Law in terms of the stress tensor (see, *e.g.*, Landau & Lifshitz 1959, p. 11).

$$\mathbf{T}_{ij} = -p\delta_{ij} + \sigma_{ij} \quad (4)$$

$$\sigma_{ij} = 2\mu u_{ij}, \quad (5)$$

where p is the isotropic pressure, μ is the elastic shear modulus, σ_{ij} represents the contribution of the material's rigidity to the stress, and we have applied eq. (3).

We consider an initial configuration in which the material is under great internal pressure but unstrained ($u_{ij} = 0$). The equation of hydrostatic equilibrium is then

$$-\nabla p_0 - \rho \nabla \phi_0 = \mathbf{F}_0, \quad (6)$$

and, in the limit of slow rotation, $R\Omega/v_k \ll 1$, F_0 is small compared to both ∇p_0 and $\rho \nabla \phi_0$.

To derive the condition for hydrostatic equilibrium in the new configuration produced by the change in \mathbf{F} , we consider a Lagrangian perturbation of the initial state. A Lagrangian perturbation Δ is evaluated moving with the matter, and is related to an Eulerian perturbation δ through

$$\Delta = \delta + \mathbf{u} \cdot \nabla. \quad (7)$$

A Lagrangian perturbation commutes with spatial derivatives as (see, *e.g.*, Shapiro & Teukolsky 1983; p. 131)

$$\Delta \frac{\partial}{\partial x_i} = \frac{\partial}{\partial x_i} \Delta - \frac{\partial u_j}{\partial x_i} \nabla_j. \quad (8)$$

We obtain the new equilibrium by taking a Lagrangian perturbation of eq. (2), *i.e.*,

$$\Delta [\nabla \cdot \mathbb{T} - \rho \nabla \phi = \mathbf{F}]. \quad (9)$$

Using eqs. (1) through (6), we obtain,

$$-\nabla \Delta p - \rho c_t^2 \nabla \times \nabla \times \mathbf{u} - \rho \nabla \delta \phi = \delta \mathbf{F} - \nabla (\mathbf{u} \cdot \nabla p_0) + (\mathbf{u} \cdot \nabla) \mathbf{F}_0 - \mathbf{u}_k \frac{\partial F_k}{\partial x_i}, \quad (10)$$

where we have neglected terms of order \mathbf{u}^2 and $c_t = \sqrt{\mu/\rho}$ is the transverse sound speed, which we take to be constant throughout the solid. For the case of slow rotation, $R\Omega/v_k \ll 1$, the last two terms in eq. (10) are smaller than the leading terms by a factor $\sim (\Omega R/v_k)^2$, and we neglect them.

We express the Eulerian change in centrifugal force by means of a scalar potential χ defined as

$$\delta\mathbf{F} = \rho\nabla\chi. \quad (11)$$

Introducing a second potential h ,

$$c_t^2 h \equiv -\frac{1}{\rho}\Delta p - \delta\phi - \chi + \frac{1}{\rho}\mathbf{u} \cdot \nabla p_0, \quad (12)$$

we rewrite eq. (10) as

$$\nabla \times \nabla \times \mathbf{u} = \nabla h. \quad (13)$$

Taking the divergence of this equation, we see that the potential satisfies

$$\nabla^2 h = 0. \quad (14)$$

The displacement \mathbf{u} is obtained by solving eqs. (13) and (14) with (12) subject to boundary conditions.

3.2. Displacement Field of the Crust

In a spherical coordinate system (r, θ) with $\mathbf{\Omega}$ directed along the z -axis, the centrifugal potential associated with a change in rotation rate $\delta\Omega$ is

$$\chi \equiv \frac{2}{3}\Omega\delta\Omega r^2(1 - P_2(\theta)), \quad (15)$$

where $P_2 = (3\cos^2\theta - 1)/2$ is the second Legendre polynomial. The $P_2(\theta)$ symmetry of χ suggests a solution to eq. (14) of the form

$$h(r, \theta) = \left(Ar^2 + \frac{B}{r^3} \right) P_2(\theta) + C, \quad (16)$$

where A , B and C are constants. For the displacement field, we seek a solution of the form

$$u_r(r, \theta) = f(r)P_2(\theta) \quad (17)$$

$$u_\theta(r, \theta) = g(r)\frac{dP_2(\theta)}{d\theta} \quad (18)$$

where $f(r)$ and $g(r)$ are functions of depth in the star only. The solution to eqs. (13) and (14), with (16), and subject to condition (3), is

$$u_r(r, \theta) = \left(ar - \frac{A}{7}r^3 - \frac{B}{2r^2} + \frac{b}{r^4} \right) P_2(\theta) \quad (19)$$

$$u_\theta(r, \theta) = \left(\frac{ar}{2} - \frac{5}{42}Ar^3 - \frac{b}{3r^4} \right) \frac{dP_2(\theta)}{d\theta}, \quad (20)$$

where a and b are additional constants. We require four boundary conditions to specify the four coefficients.

3.3. Boundary Conditions

At the outer boundary the crust encounters a vacuum, while at the inner boundary it is in contact with the liquid core. Since neither of these media support traction, two boundary conditions follow from requiring that no shear exist at each boundary, *i.e.*,

$$\sigma_{r\theta} = 0 \quad \text{at} \quad r = R, R', \quad (21)$$

or,

$$\frac{\partial u_\theta}{\partial r} - \frac{u_\theta}{r} + \frac{1}{r} \frac{\partial u_r}{\partial \theta} = 0 \quad \text{at} \quad r = R, R'. \quad (22)$$

In terms of the coefficients

$$a - \frac{8}{21}AR^2 - \frac{B}{2R^3} + \frac{8}{3} \frac{b}{R^5} = 0 \quad (23)$$

$$a - \frac{8}{21}AR'^2 - \frac{B}{2R'^3} + \frac{8}{3} \frac{b}{R'^5} = 0. \quad (24)$$

Two other boundary conditions follow from requiring that the material be in mechanical equilibrium at the boundaries. This requirement is satisfied by ensuring that

$$\mathbb{T}_{rr} = -p + \sigma_{rr}, \quad (25)$$

is continuous at $r = R, R'$. Hence,

$$\left[-\Delta p + 2\rho c_t^2 \frac{\partial u_r}{\partial r} \right]_{r=R-\varepsilon} = 0, \quad (26)$$

$$\left[-\Delta p + 2\rho c_t^2 \frac{\partial u_r}{\partial r} \right]_{r=R'+\varepsilon} = [-\Delta p]_{r=R'-\varepsilon}, \quad (27)$$

where ε is an infinitesimal positive distance. We have required $\Delta p = 0$ just above the star and have taken $c_t = 0$ in the liquid core. These jump conditions specify the material stress required to maintain a pressure difference across a boundary.

The local pressure change follows from eq. (12)

$$\Delta p = -\rho c_t^2 h - \rho \delta\phi - \rho\chi + \mathbf{u} \cdot \nabla p_0. \quad (28)$$

The initial, unstrained configuration is that of a Maclaurin spheroid whose shape, for small eccentricity e , can be written

$$R(\theta) = R \left[1 - \frac{1}{3} e^2 P_2(\theta) \right] \equiv R + \epsilon(\theta). \quad (29)$$

The gravitational potential for a slowly-rotating Maclaurin spheroid is (Shapiro & Teukolsky 1983, *Black Holes, White Dwarfs and Neutron Stars*, p. 169)

$$\phi = -\pi G \rho \left[2R^2 - \frac{2}{3} r^2 + \frac{4}{5} \frac{r^2}{R} \epsilon(\theta) \right]. \quad (30)$$

Since the crust of a neutron star contains only $\sim 1\%$ of the star's mass, we neglect the crust's effect on the gravitational potential. As the star spins down, ϵ changes by $u_r(R, \theta)$.

Hence, the *Eulerian* change in the potential is

$$\delta\phi = -\frac{4}{5} \pi G \rho \frac{r^2}{R} u_r(R, \theta). \quad (31)$$

For slow rotation, ∇p_0 is nearly radial, and we may approximate the last term in eq. (28) as

$$\mathbf{u} \cdot \nabla p_0 \simeq -\rho u_r(r, \theta) \nabla\phi_0 \simeq -\frac{4}{3} \pi G \rho^2 r u_r(r, \theta), \quad (32)$$

where we used the spherical (non-rotating) gravitational potential in the last step, which is justified in the limit of slow rotation.

Combining eqs. (28), (31), (32), and (15) through (17), the boundary condition (26) at the surface yields

$$-2f'(R) - \frac{2v_k^2}{5c_t^2} \frac{f(R)}{R} + \frac{2\Omega\delta\Omega R^2}{3c_t^2} = AR^2 + \frac{B}{R^3}, \quad (33)$$

where $f(R)$ is defined by eq. (19) and $v_k^2 \equiv 4\pi GR^2\rho/3$.

To match the solutions at the crust-core boundary, we require an expression for the pressure change in the core. We obtain it from eq. (10) setting $c_t = 0$ since a liquid cannot support shear. We have

$$\nabla \left[-\frac{\Delta p}{\rho} - \delta\phi + \frac{1}{\rho} \mathbf{u} \cdot \nabla p_0 - \chi \right] = 0. \quad (34)$$

Hence,

$$-\frac{\Delta p}{\rho} - \delta\phi + \frac{1}{\rho} \mathbf{u} \cdot \nabla p_0 - \chi = \text{constant} \quad (35)$$

in the core. The pressure change in the shell obeys

$$-\frac{\Delta p}{\rho} - \delta\phi + \frac{1}{\rho} \mathbf{u} \cdot \nabla p_0 - \chi = c_t^2 \left[Ar^2 + \frac{B}{r^3} \right] P_2(\theta) + C. \quad (36)$$

Thus, the boundary condition (27) at the crust-core boundary, using eqs. (35) and (36), gives

$$\left[\frac{\partial u_r}{\partial r} \right]_{r=R'+\varepsilon} = -\frac{1}{2} \left[AR'^2 + \frac{B}{R'^3} \right] P_2(\theta) + \text{constant}. \quad (37)$$

From the form assumed for u_r , we see that the constant is zero. We finally obtain

$$f'(R') = -\frac{1}{2} \left[AR'^2 + \frac{B}{R'^3} \right]. \quad (38)$$

Eqs. (19), (20), and the boundary conditions (23), (24), (33) and (38) complete the description of the displacement field driven by a change in rotation rate $-\delta\Omega$.

Recent calculations with realistic equations of state suggest that neutron stars have crusts of thickness $0.05 - 0.08R$ (Akmal *et al.* 1998; Lorenz *et al.* 1993); in the following, we take $t \equiv R - R' = 0.05R$. The corresponding displacement field is shown in Fig. 2. From the displacement field we can calculate the strain distribution resulting from spin down. The strain tensor (1) can be diagonalized to obtain the strain angle and the planes along which the material can shear. The geometry of crust cracking can be obtained from an analysis of the distribution of strain angles over the crust, to which we now turn.

4. Cracking the Crust

As the star spins down and the strain increases, the crust breaks when the local strain angle reaches a critical value. Fig. 3 shows contours of constant strain angle through the crust; the strain angle is maximum at the crust-core boundary, in the equatorial plane. Fig. 4 shows the three eigenvalues of the strain tensor at the inner boundary of the crust plotted as a function of latitude. The strain angle, shown by the darker curve, shows discontinuous derivatives where the maximum and minimum eigenvalues change. The dashed curve corresponds to the strain angle for a homogeneous elastic sphere model (LFE) at the same depth for comparison. In the equatorial plane ($\theta = \pi/2$), the stress plane is the $\theta\phi$ -plane. An element of matter on the equatorial plane is compressed by adjacent elements on the equator and expands in the r and θ directions. Material compressed in this way shears along one of two planes that takes an angle of $\gamma \sim 30 - 45^\circ$ with respect to the compressive force (Green & Houston 1995; see Fig. 1). Once the crust breaks, matter moves along faults F or F' , inclined at an angle γ to the rotational equator (see Fig. 6). Since the strain field has azimuthal symmetry, the break is equally likely to begin at all points on a ring corresponding to the intersection of the crust core boundary with the equatorial plane. The inclusion of magnetic stresses, discussed below, breaks this symmetry.

The propagation of the crack is a nonlinear process; cracking affects the strain field, which in turn affects the propagation of the crack. In general, cracking increases the stress on unbroken neighboring material (Hertzberg 1996), causing the fault plane to grow in both width and length. Hence, the crack begins at the base of the crust in the equatorial plane, propagates toward the surface, and continues to grow up to some latitude. When the cracking ends, the strain field is everywhere subcritical. The width and length of the fault plane cannot be determined from the linear analysis given here.

In this treatment, we have ignored the fact that the neutron star crust is stratified. Inspection of eq. [10] shows that the most important material property controlling the development of strain is c_t ; in particular, where c_t is small, the strain must be large. Strohmayer (*et al.* 1991) calculated c_t as a function of density in the neutron star crust and found that it varies by a factor of $\sim 10^2$. Cracking of the crust is favored in regions where c_t is small, possibly causing the quake epicenter to be somewhat higher than the base of the crust. We expect that the effects of density stratification will not affect the overall geometry of crust cracking described here.

5. Magnetic stresses

We now examine the effects of the magnetic field that is anchored to the crust of the neutron star. The displacements induced by the spin down distort the magnetic field, generating magnetic stresses. If the magnetic field is not precisely aligned with the rotation axis, the magnetic stresses will break the azimuthal symmetry of the strain distribution in the crust.

A complete description of the strain field that develops in magnetized material is obtained by solving the elasticity equations and Maxwell's equations self-consistently,

subject to boundary conditions at the star’s surface. The surface boundary conditions, however, are complex to handle; in a realistic neutron star they depend on the exact form of the density gradients near the surface. To qualitatively illustrate the influence of the star’s magnetic field on where starquakes originate and how they propagate, we consider the simpler problem of the magnetic fields effect on the material strain in an unbounded medium.

In the absence of the field, the equilibrium state is given by

$$\frac{\partial \sigma_{ij}}{\partial x_i} + F_j = 0, \quad (39)$$

where F_j represents gravitational and centrifugal forces. The presence of a magnetic field introduces several forces. First, the unperturbed field can exert a force on the crust. For this study, we assume that the initial field \mathbf{B} is dipolar and hence force free; that is, the unperturbed Maxwell stress tensor \mathbb{T}_{ij} obeys $\partial \mathbb{T}_{ij} / \partial x_i = 0$ in the crust. Next, the displacement field in the crust distorts the field by $\delta \mathbf{B}$, generating a perturbation $\delta \mathbb{T}_{ij}$ to the Maxwell stress tensor.³ The new equilibrium is given by

$$\frac{\partial}{\partial x_i} (\delta \sigma_{ij} + \delta \mathbb{T}_{ij}) = 0 \quad (40)$$

where $\delta \sigma_{ij}$ is the magnetically induce change in the material stress tensor. For an infinite medium (or a finite one in which boundary effects are unimportant), the solution is $\delta \sigma_{ij} = -\delta \mathbb{T}_{ij}$.

Magnetic stresses modify the displacement \mathbf{u} by $\delta \mathbf{u}$. For a magnetic field that is sufficiently small that this correction to the displacement field is small ($|\delta \mathbf{u}| \ll |\mathbf{u}|$), the

³The ratio of magnetic to material stresses is $\sim \beta \equiv (v_A/c_t)^2$ where v_A is the Alfvèn speed and c_t is the transverse sound speed. In the outer crust, we have $\beta = 8 \times 10^{-4} (B/10^{12} \text{ G})^2 (\rho/10^{10} \text{ g cm}^{-3})^{-1} (c_t/10^8 \text{ m s}^{-1})^{-2}$ and we are justified in treating the magnetic effects perturbatively.

perturbation to the Maxwell stress tensor is

$$\delta\mathbb{T}_{ij} = \frac{1}{4\pi} [\delta B_i B_j + B_i \delta B_j - B_k \delta B_k \delta_{ij}], \quad (41)$$

with

$$\delta\mathbf{B} = \nabla \times (\mathbf{u} \times \mathbf{B}). \quad (42)$$

Here \mathbf{u} is the displacement field in the absence of the magnetic field. For incompressible matter, the correction δu_{ij} to the strain tensor is

$$\delta u_{ij} = \frac{1}{2\mu} \left(\delta \sigma_{ij} - \frac{1}{3} \delta \sigma_{ll} \delta_{ij} \right), \quad (43)$$

where μ is the shear modulus. The eigenvalues of this tensor give the correction to the strain angle due to the induced magnetic forces. Using the displacement field of eqs. (19) and (20) in eq. (42), we obtain an estimate of the corrections to the strain angle on the star’s rotational equator; these are shown in Fig. 5.

The magnetic field affects our picture of crust cracking in two ways. First, the existence of the magnetic field strengthens the material, making it harder to shear. The material is weaker and hence most likely to shear where the magnetic field is weakest. Consider a star with a dipolar magnetic field inclined at an angle α to the rotation axis. In this case the material may begin shearing at the two points on the rotational equator that are farthest away from the magnetic poles as shown in the schematic of Fig. 6. Second, as the material attempts to move along the fault planes, the magnetic field opposes displacements that cross field lines and hence favors matter motion long fault F over fault F' . This motion moves matter closer to the magnetic poles. This picture is essentially the same as found for a simpler homogeneous sphere model (LFE).

6. Discussion

We have examined the evolution of strain in the crust of an idealized spinning-down neutron star and the initiation of starquakes as the material reaches critical strain. We modeled the neutron star as a self-gravitating core of incompressible liquid that supports a brittle crust. Crust cracking occurs as material shears under the compressive forces arising from the star’s decreasing circumference. The star initially cracks near the star’s rotational equator, at the base of the crust. The shearing motion along the fault decreases the oblateness of the star and pushes matter to higher latitudes. Magnetic stresses suppress shearing near the magnetic poles and across the field lines. Starquakes thus originate near the two points on the equator farthest from the magnetic poles and propagate toward the magnetic poles. Our conclusion is qualitatively the same as found in our simpler homogeneous spherical model (LFE).

As material slides along a fault directed toward the magnetic poles, the star’s principal axis of inertia shifts *away* from the magnetic axis, exciting precession. Eventually, damping restores alignment between the principal axis of inertia and the angular momentum axis, increasing the angle between the rotation and magnetic axes. In some models of pulsar spin-down, *e.g.*, the magnetic dipole model, this growth in the alignment angle increases the spin-down torque. We might, therefore, expect to see a tendency of alignment angle to increase with age in young pulsars. In older pulsars, however, Tauris & Manchester (1998), find no relationship between magnetic alignment angle and spin-down torque.

One possible observational signature from a starquake is a change of the pulse profile. A jump in the alignment angle α changes the duration of the line of sight’s traverse through the pulse emission cone. In the Crab pulsar, the relative change in pulsed flux could be of order 1% (Link & Epstein 1997). Additionally, the energy released in a starquake could produce an observable enhancement of the star’s luminosity. The energy release is of

order $E \sim 10^{42}(\mu/10^{31} \text{ erg cm}^{-3})(d/10^5 \text{ cm})^3(\theta_c/10^{-2})^2$ ergs, where μ is the average shear modulus along a fault of length d and θ_c is the strain angle at which fracture occurs. Some fraction of the seismic energy will be damped, heating the crust. Eventually, a soft x-ray thermal wave will emerge from the star's surface. For localized deposition of 10^{42} ergs at a density of $10^{14} \text{ g cm}^{-3}$, Tang (1999) calculates a 5% enhancement of the star's luminosity occurring about 3 yr after the quake for a star with an internal temperature of 10^7 K and a stiff equation of state. For deposition at $10^{13} \text{ g cm}^{-3}$ in a star with an internal temperature of 10^8 K, the enhancement is $\sim 22\%$. The Chandra X-ray Observatory should be capable of detecting this enhancement in a closer source, such as the Vela pulsar.

A starquake could drive non-thermal emission as well. Seismic energy that reaches the stellar surface couples to Alfvén waves which propagate into the magnetosphere. Conversion of Alfvén waves into γ -rays could occur if the waves are charge-starved or if their amplitudes are comparable to the background field strength of the magnetosphere (Blaes *et al.* 1989).

We thank A. Olinto for valuable discussions and C. Miller for a critical reading of the manuscript. This work was performed under the auspices of the U.S. Department of Energy, and was supported in part by NASA EPSCoR Grant #291748, NASA ATP grant # NAG 53688, by IGPP at LANL and by the Center for Thermonuclear Flashes at the University of Chicago.

REFERENCES

- Akmal, A., Pandharipande, V. R. & Ravenhall, D. G. 1998, *Phys. Rev. C*, 58, 1804
- Baym, G. & Pines, D. 1971, *Ann. Phys.*, 66, 816
- Blaes, O., Blandford, R., Goldreich, P. & Madau, P. 1989, *ApJ*, 343, 839
- Chandrasekhar, S. 1987, *Ellipsoidal Figures of Equilibrium* (New York, NY: Dover)
- Cheng, B. L, Epstein, R. I., Guyer, R. A. & Young, A. C. 1996, *Nature*, 382, 518-520
- Duncan, R. C. & Thompson, C. 1994, in *Gamma-ray Bursts*, Am. Inst. Phys., New York, (eds: Fishman, G. J., Brainerd, J. J., Hurley, K.), p. 625
- Gogus, E., Woods, P. E., Kouveliotou, C., van Paradjis, J., Briggs, M. S., Duncan, R. C., & Thompson, C. 1999, *ApJ*, in press (astro-ph/9910062)
- Green, H. W. II & Houston, H. 1995, *Ann. Rev. Earth Planet Sci.*, 23, 169
- Hertzberg, R. W. 1996, *Deformation and Fracture Mechanics of Engineering Materials*, (New York: Wiley)
- Landau, L. D. & Lifshitz, E. M. 1959, *Theory of Elasticity*, (London: Pergamon Press)
- Link, B., and Epstein, R. I. 1996, *ApJ*, 457, 844
- Link, B., and Epstein, R. I. 1997, *ApJ*, 478, L91
- Link, B., Franco, L. M. & Epstein, R. I. 1998, *ApJ*, 508, 838
- Lorenz, C. P., Ravenhall, D. G. & Pethick, C. J. 1993, *Phys. Rev. Lett.*, 70, 379
- Lyne, A. G., Pritchard, R. S., & Smith, F. G. Smith 1993, *MNRAS*, 265, 1003
- Ruderman, M. 1976, *ApJ*, 203, 213

- Shapiro, S. L. & Teukolsky, S. A. 1983, *Black Holes, White Dwarfs, and Neutron Stars*,
(New York: Wiley)
- Shemar, S. L. & Lyne, A. G. 1996, *MNRAS*, 282, 677
- Strohmayer, T., Ogata, S., Iyemori, H., Ichimaru, S., & Van Horn, H. M. 1991, *ApJ*, 375,
679
- Tang, A. 1999, M.S. Thesis, University of Hong Kong
- Tauris, T. M., & Manchester, R. N. 1998, *MNRAS*, 298, 625
- Thompson, C. & Blaes, O. 1998, *Phys. Rev. D*, 57, 3219
- Thompson, C. & Duncan, R. C. 1995, *MNRAS*, 275, 255
- Thompson, C. & Duncan, R. C. 1996, *ApJ*, 473, 322

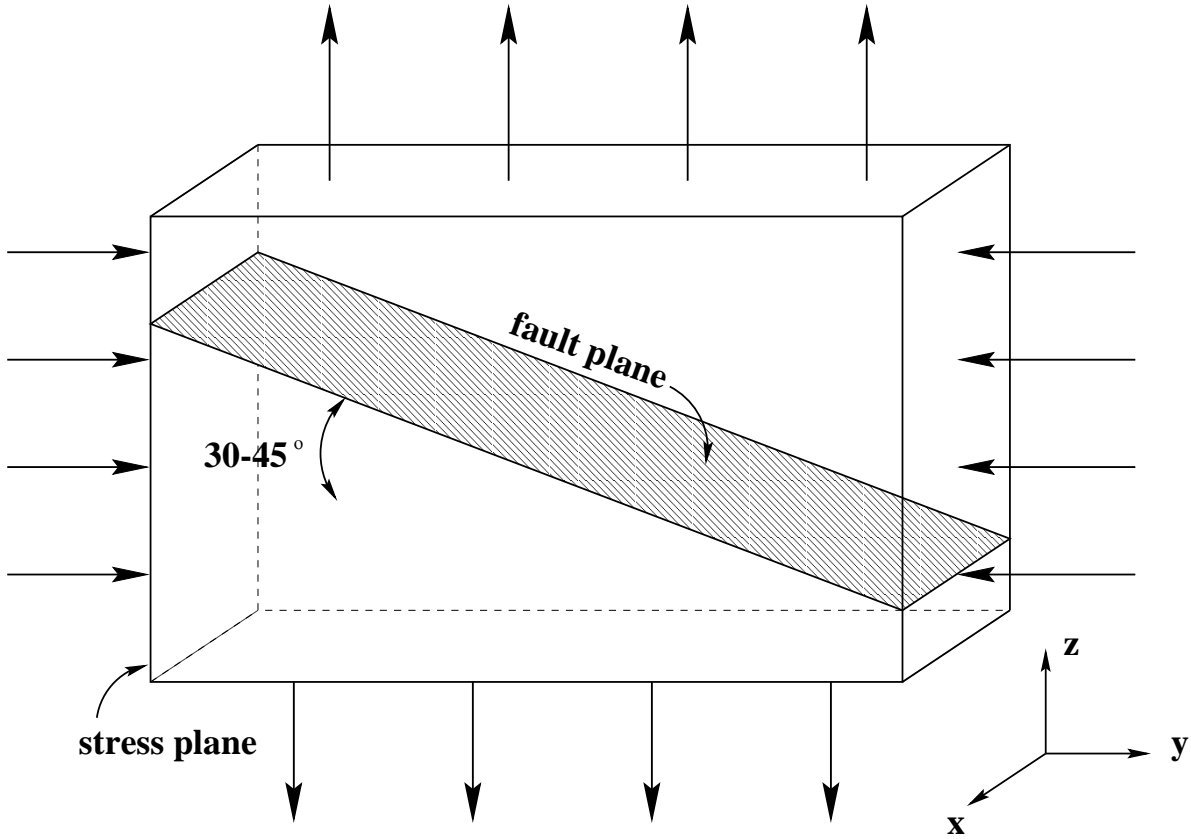


Fig. 1.— Breaking of a compressed matter element. A block of matter subjected to horizontal compression and vertical tension shears along a fault plane as shown when critical strain is reached. Shearing along a complementary plane flipped over with respect to the plane shown is equally likely for isotropic material. The y - z plane is the *stress plane*.

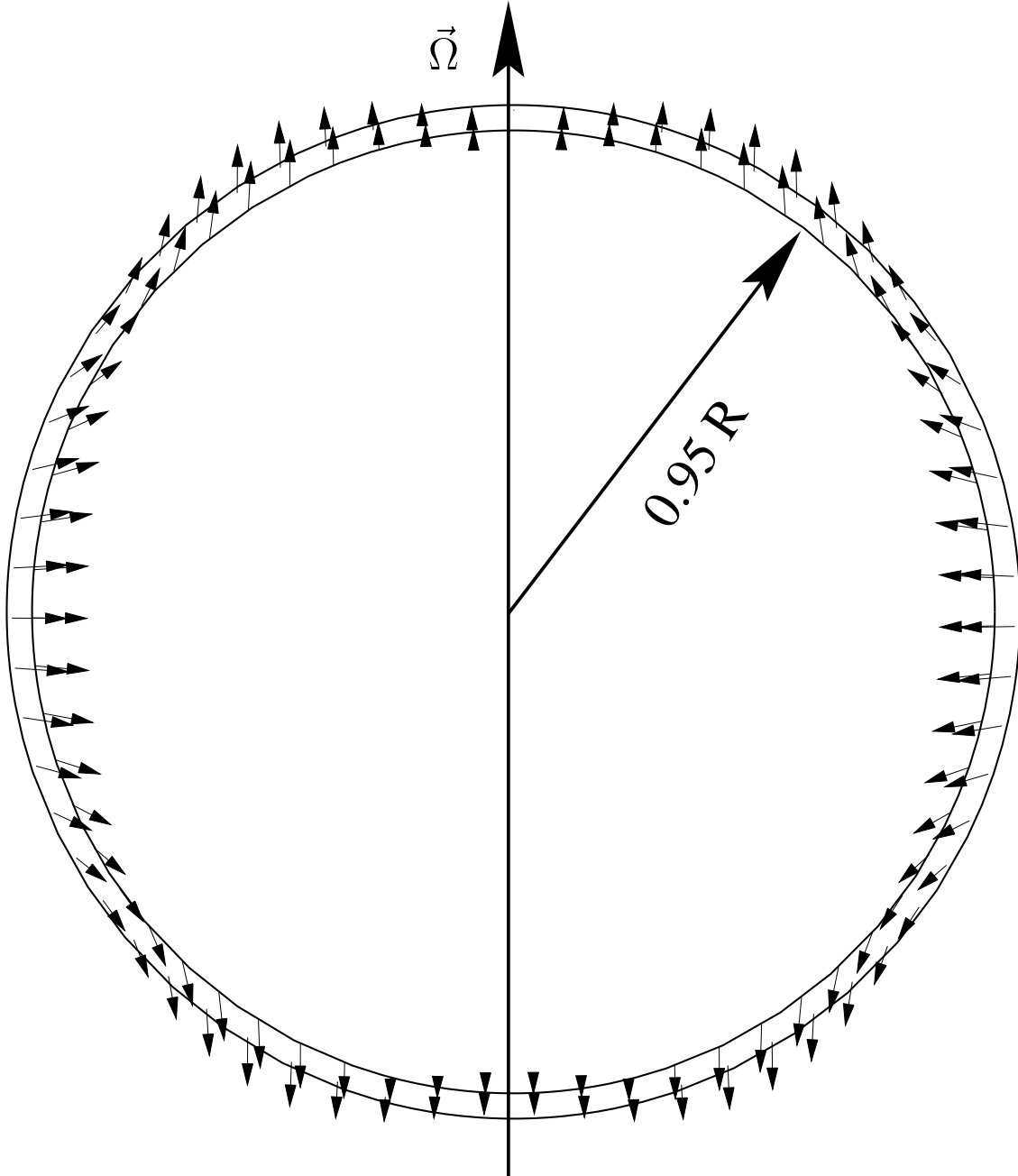


Fig. 2.— The displacement field in a spinning-down neutron star. A cross section through the center of the star is shown for a model with relative crust thickness of 5%. The equatorial diameter decreases while the polar diameter increases.

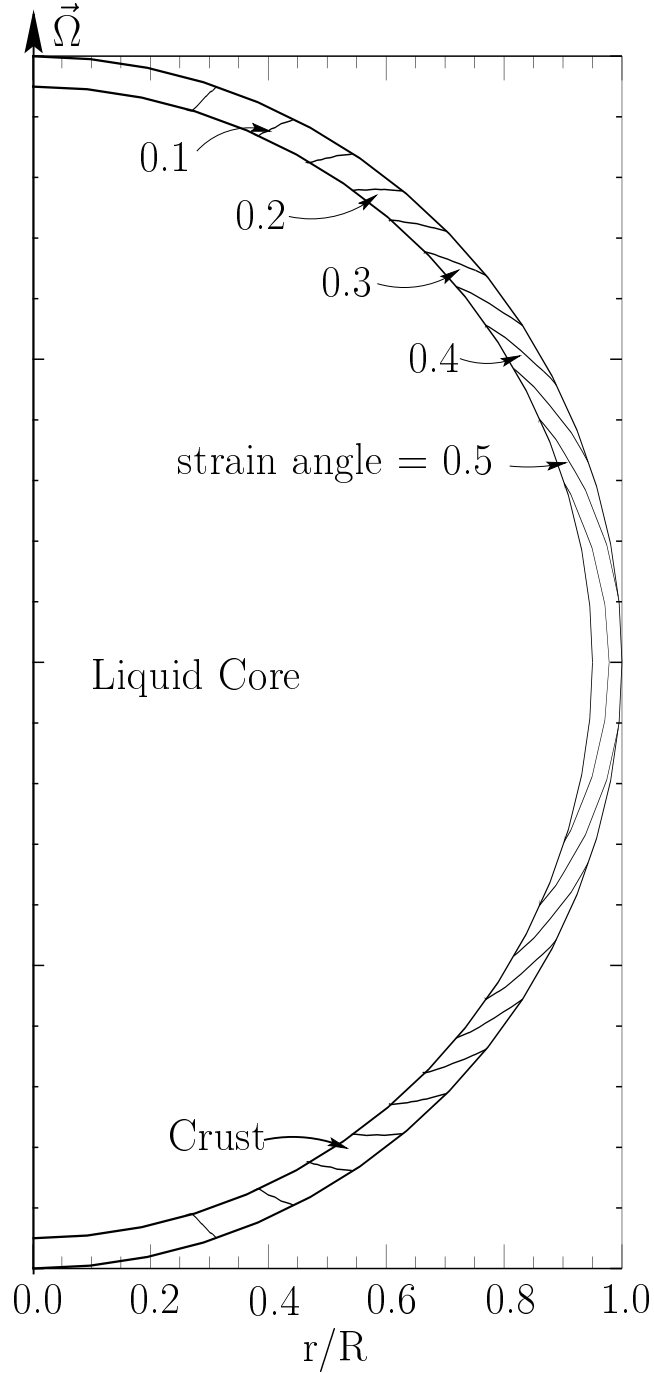


Fig. 3.— Contours of constant strain angle as a function of depth in the crust for a non-magnetized neutron star (arbitrary units). The maximum strain angle occurs at the equator and on the inner boundary of the stellar crust.

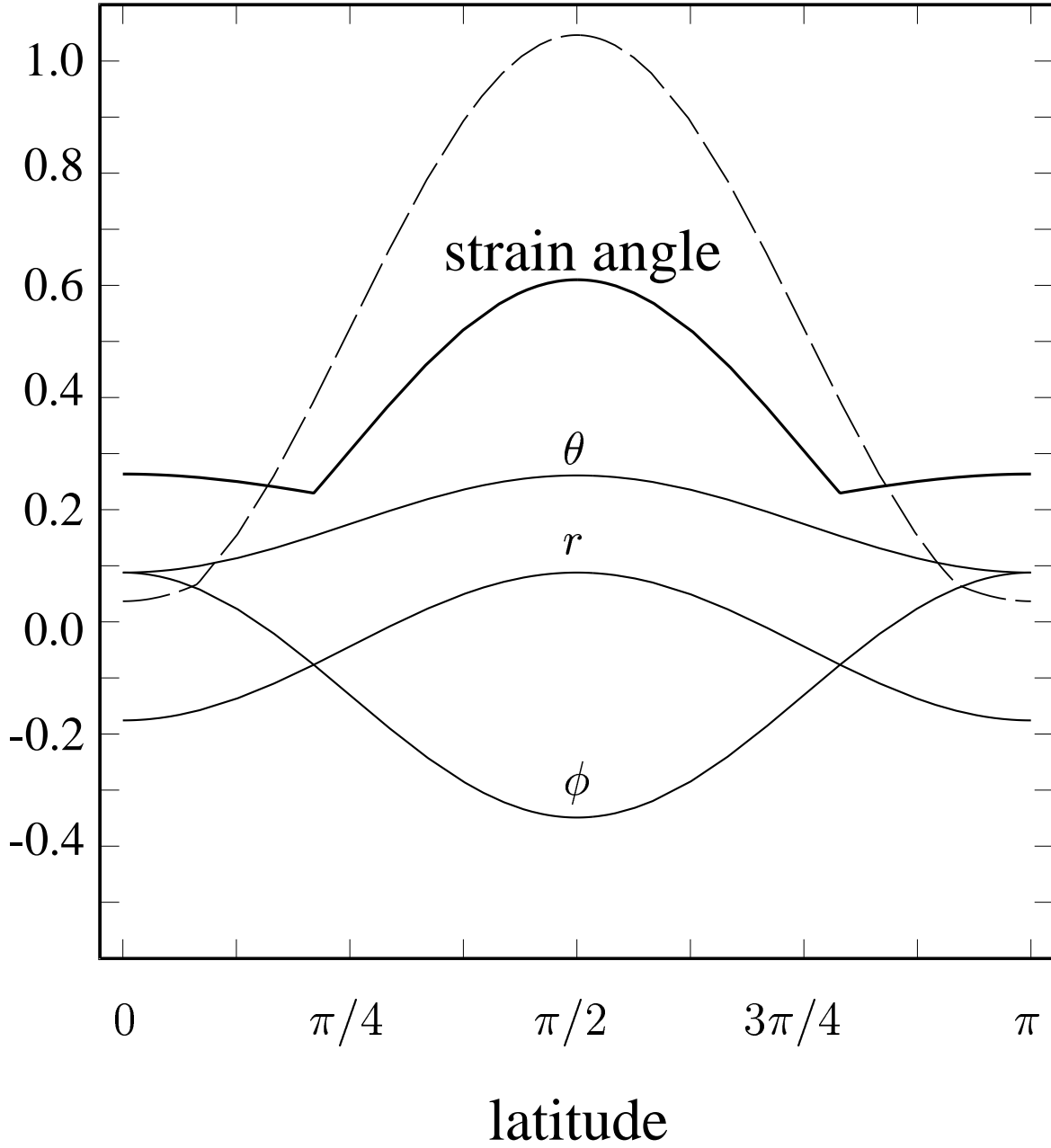


Fig. 4.— Strain eigenvalues and strain angle vs. latitude at the stellar surface for $B = 0$ (arbitrary units). The curves show the strain angle and the eigenvalues as marked. The dashed line corresponds to the strain angle for the homogeneous sphere of LFE.

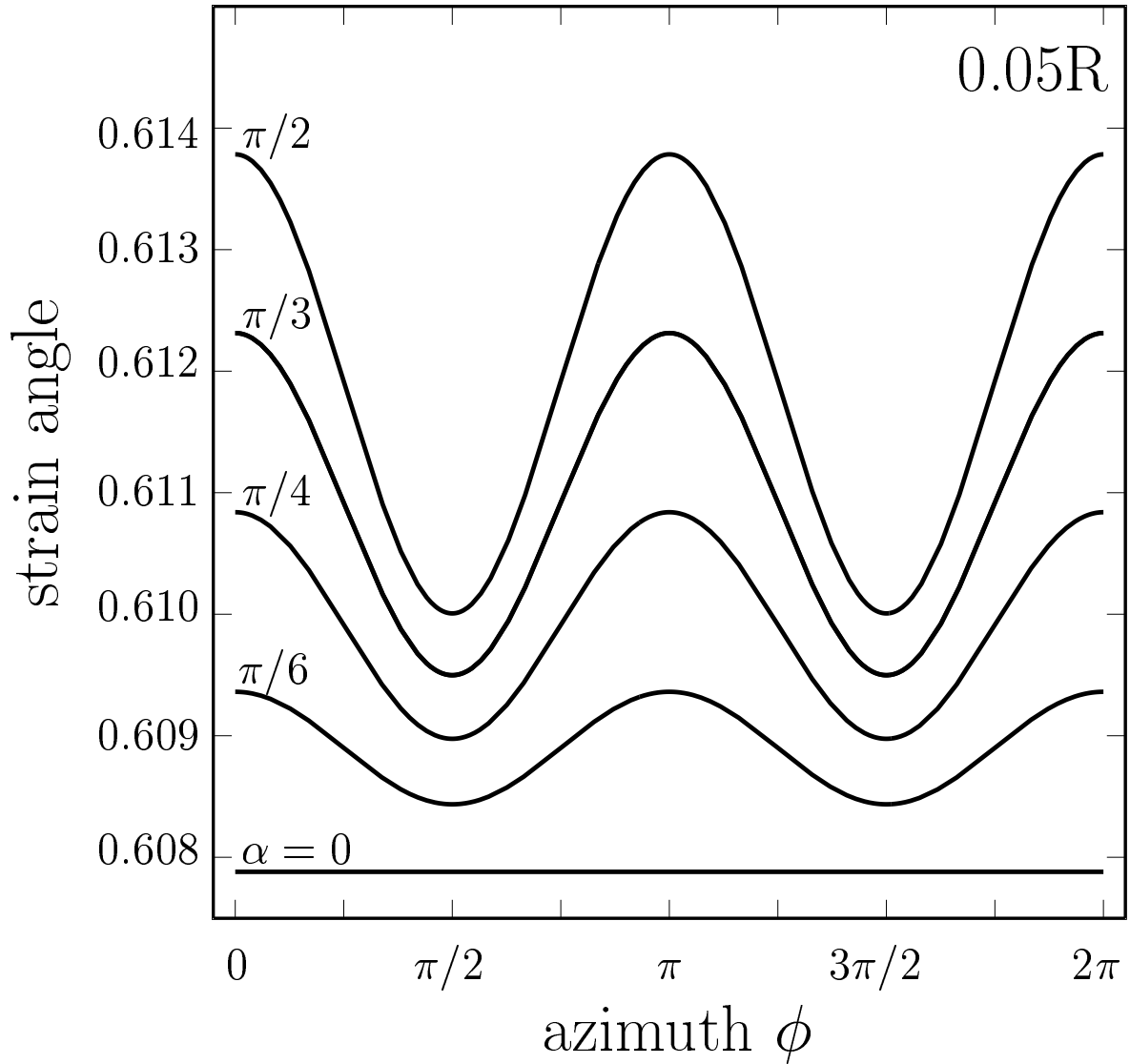


Fig. 5.— The strain angle of surface equatorial material in the presence of a magnetic field (arbitrary units). The curves correspond to different values of the angle α between the magnetic and rotation axes. The magnetic poles are at azimuthal angles $\pi/2$ and $3\pi/2$.

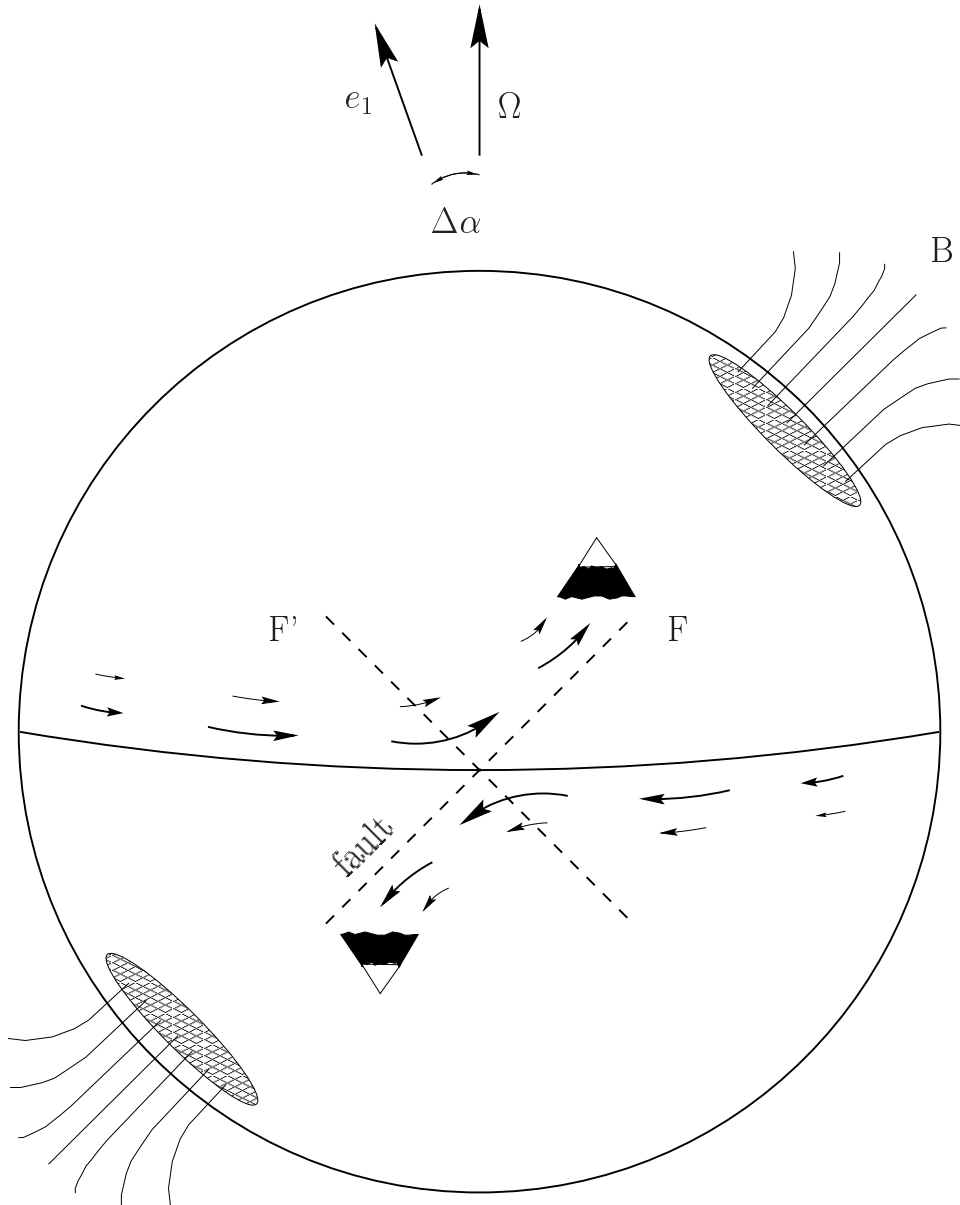


Fig. 6.— A starquake. In the absence of a magnetic field, the material is equally likely to begin breaking along faults F and F' , anywhere on the equator. These fault planes are perpendicular to the stellar surface. In the presence of magnetic stresses, fault F is more likely, creating “mountains” (indicated by the snow-capped peaks) and shifting the largest principal axis of inertia to a new direction e_1 (fixed in the star).